

# Interfacing Foundation Models' Embeddings

Xueyan Zou<sup>\*§♣</sup>, Linjie Li<sup>\*#</sup>, Jianfeng Wang<sup>#</sup>, Jianwei Yang<sup>#</sup>, Mingyu Ding<sup>‡</sup>, Zhengyuan Yang<sup>#</sup>  
 Feng Li<sup>†</sup>, Hao Zhang<sup>†</sup>, Shilong Liu<sup>&</sup>, Arul Aravinthan<sup>§</sup>, Yong Jae Lee<sup>§¶</sup>, Lijuan Wang<sup>#¶</sup>  
<sup>§</sup> UW-Madison <sup>#</sup> Microsoft <sup>‡</sup> UC Berkeley <sup>†</sup> HKUST <sup>&</sup> Tsinghua University  
<sup>¶</sup> Equal Advisory Contribution <sup>♣</sup> Main Technical Contribution <sup>\*</sup> Equal Contribution

[x-decoder-vl.github.io](https://github.com/UX-Decoder/vl)



Figure 1. The proposed *FIND* interface is generalizable to tasks that span granularity (pixel to image) and modality (vision to language) with an interleaved representation space. Apart from the in-domain tasks of generic segmentation, interactive segmentation, grounded segmentation, interleaved segmentation, and image-text retrieval, our approach is generalizable to zero-shot tasks including cross-image interleave retrieval and text grounding. All the results in the teaser figure are predicted by *FIND*-Large, and the retrieval dataset for the teaser figure includes coco\_val2017 and new images generated by DALLE-3.

## Abstract

We present *FIND*, a generalized interface for aligning foundation models' embeddings. As shown in Fig. 1, a lightweight transformer interface without tuning any foundation model weights is enough for a unified image (segmentation) and dataset-level (retrieval) understanding. The proposed interface has the following favorable attributes: (1) *Generalizable*. It applies to various tasks spanning retrieval, segmentation, etc., under the same architecture and weights. (2) *Prototypable*. Different tasks are able to be implemented through prototyping attention masks and embedding types. (3) *Extendable*. The proposed interface is

*adaptive to new tasks, and new models.* (4) *Interleavable*. With the benefit of multi-task multi-modal training, the proposed interface creates an interleaved shared embedding space. In light of the interleaved embedding space, we introduce the *FIND*-Bench, which introduces new training and evaluation annotations to the COCO dataset for interleave segmentation and retrieval. Our approach achieves state-of-the-art performance on *FIND*-Bench and competitive performance on standard retrieval and segmentation settings. The training, evaluation, and demo code as well as the dataset have been released at <https://github.com/UX-Decoder/FIND>.

## 1. Introduction

With the exhilarating progress in foundation models across the vision and language domains, such as GPT4(V) [29], DALLE-3 [28], SAM [17], and LLaMA [34], *etc.*, we have reached a stage where deep learning models achieve remarkable performances on both vision and language domains [4, 20].

However, the process of training individual foundation models has become remarkably costly in both energy expenditure and the utilization of human resources. Furthermore, the full potential of these models remains untapped due to limitations in their fixed output modalities (i.e. text output for Q&A and visual output for image generation). Although techniques such as prompt engineering [41] and adaptive tuning [37] have shown promising results in enhancing output quality or better in-domain task performance, these approaches struggle with integrating different foundation models (i.e. SAM, LLaMA) off the shelf, expanding the output types (i.e., text, image, pixel) and task objectives (i.e., from Q&A to retrieval and segmentation).

In light of these observations, we aim to build an INterface for Foundation models’ embeDDings (*FIND*). The interface enables task-adaptive prototyping, which means we only need to change the configure file instead of the model architecture when adapting to the new tasks. Because all the vision-language tasks are trained in a unified way, this creates an **interleaved share embedding space** where vision and language references are replaceable and addable. For example, as shown in Fig. 1, we can handle queries, in which text and image jointly describe one scenario. Moreover, we expect that such an interface can leverage the pre-trained foundation models from different modalities. For example, by interfacing SAM and LLaMA, we can connect SAM features with semantic meanings.

Our interface is built upon frozen foundation models, the vision encoder provides semantic-aware and object-sensitive features, and the language encoder predicts semantic and logic-aware features. Therefore, the proposed interface is used for distilling information from the foundation model features for downstream tasks. In this context, we denote the features as the unsampled output of foundation models (before the embedding sampler of Fig. 2).

The proposed method differs from previous multi-modal LLMs, such as BLIP [21] and LLaVA [24], which feeds the vision foundation model features into a language decoder, where the LLM decoder purely regards the visual features as text tokens. Differently, We align vision features with LLM features that enable more potential on model output types, and tasks. Moreover, both LLaVA and BLIP tune the language model with extra data. This may potentially break the informative and generalizable foundation models’ features. Instead of only performing text generation conditioned on visual features, we believe that LLM features are

also rich resources for other understanding tasks such as retrieval and segmentation. Thus, we will not tune any foundation models. As shown in Fig. 1, description-based segmentation (+Language Description in the first row) is one example benefit of this design choice. In addition, unlike FROMAGE [18], which uses the last layer’s feature from LLMs to align with visual features, we empirically observe that the intermediate layer features of LLMs can be more effective for both image and pixel-level understanding tasks.

*FIND* can naturally support two new tasks (Fig. 1, row 2): (i) cross-image interleaved image retrieval, and (ii) interleaved grounded segmentation. To conduct a proper evaluation and training of these novel tasks, we further build a new benchmark, *FIND*-Bench, tailored for interleaved visual or image-text understanding, based on the COCO [23] dataset.

Our contributions are summarized as follows:

- We are the first work to explore the classic understanding capabilities of LLMs at different levels of granularity and multiple modalities.
- The proposed *FIND* Interface is generalizable, flexible, and extendable to various tasks and foundation models.
- An interleaved shared embedding space is created for foundation models through the unified interface.
- We propose a new Benchmark, *FIND*-Bench that includes new training and evaluation ground truth sets for interleave segmentation and retrieval for COCO dataset.
- Our model achieves SoTA performance on interleaved image retrieval and segmentation and shows better or comparable performance on generic/interactive/grounded segmentation and image-text retrieval.

## 2. *FIND* Approach

To bridge the embedding spaces of vision and language foundation models, we develop the *FIND* Interface, which is able to seamlessly assemble multi-modal embeddings at the semantic level.

### 2.1. Preliminary

For each task supported by *FIND*, we define the inputs as  $F = \{f.a, f.b, \dots, f.z\}$ ,  $T = \{t.a, t.b, \dots, t.z\}$ ,  $P = \{p.a, p.b, \dots, p.z\}$ ,  $Q = \{q.a, q.b, \dots, q.z\}$ , where  $F, T, P, Q$  are *features*, *tokens*, *proposals*, and *queries*, respectively. The subscripts  $\{a, b, \dots, z\}$  denote the specific type for each task such as grounding proposals (*p.grounding*), class queries (*q.class*), etc. as shown in Table 1. Each task also contains two attention operations: *content attention*, and *conditional attention*. We formally define each embedding type and operation as below:

- *Features*: Image, text features that are directly predicted by foundation models.
- *Tokens*: Content embeddings that are sampled from the

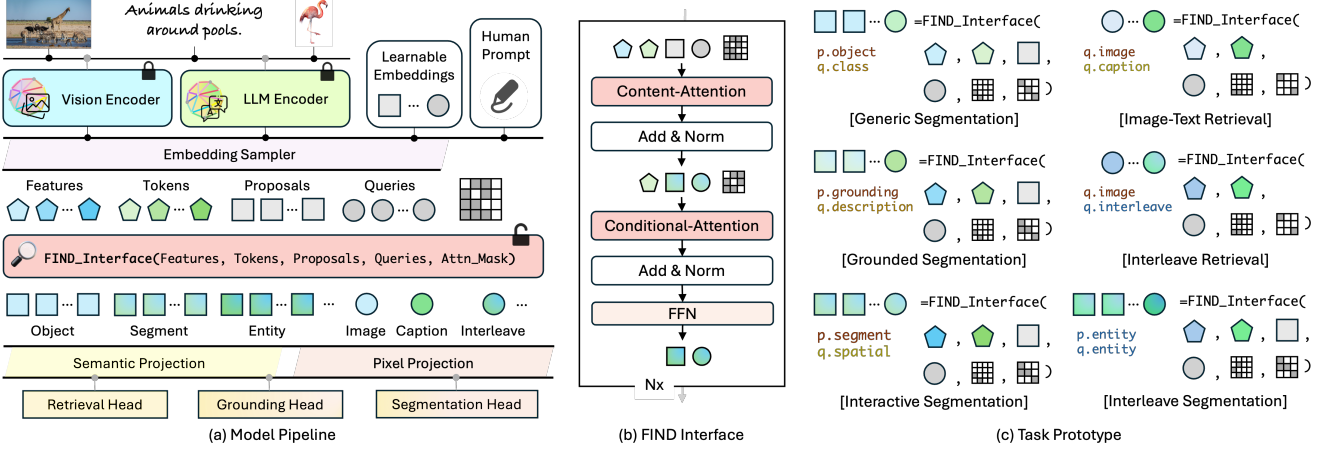


Figure 2. (a) *FIND* approach pipeline. The shape of different polygons represents different embedding types, and the color of the polygons represents different input information. (b) Detailed architecture of the *FIND* Interface. (c) Task prototype for *FIND* interface, the grid square is the attention mask for content attention and condition attention, and the mask order is the same as the input order.

image, and language features using an embedding sampler (refer to Fig. 2).

- *Proposals*: Blank embeddings that attend information from features and tokens used as the output proposals, with shape  $[n,d]$  where  $n$  is the proposal number, and  $d$  is the embedding size.
- *Queries*: Blank embeddings that attend information with features and tokens directly used for output, with shape  $[1,d]$  where  $d$  is the embedding dimension.
- *Content Attention*: Attention operations that allow proposals and queries to gather information from features and tokens given attention mask.
- *Condition Attention*: Attention operations that allow proposals to condition on specific information (e.g. token embeddings) given attention mask.

## 2.2. Pipeline

Our model is designed to interface with a pair of arbitrary vision and language foundation models.

**Embeddings Preparation** Given the input image  $I$  and input text  $T$ , the vision encoder  $\mathbf{V}$  and language encoder  $\mathbf{L}$  will encode the image and text into features, respectively:

$$f_{\text{image}} = \mathbf{V}(I), f_{\text{text}} = \mathbf{L}(T). \quad (1)$$

Similar to SEEM [50], we use an embedding sampler to sample customized vision and language tokens from features for a specific task or human prompt given the sampling coordinates  $coord$ . After sampling, we obtain  $t_{\text{image}}, t_{\text{text}} = \text{Embedding\_Sampler}(f_{\text{image}}, f_{\text{text}}, coord)$ . In addition, the embedding sampler is also responsible for sampling learnable queries and proposals from the embedding pool. Given learnable queries  $\hat{q}$  (e.g. with shape  $[1, 512]$ ), and proposals  $\hat{p}$  (e.g. with shape  $[1, 512]$ ), the task-specific queries and proposals are sampled by the indices  $idx$  through  $q_x, p_x =$

$\text{Embedding\_Sampler}(\hat{q}, \hat{p}, idx)$ . The embedding sampler is an interpolation or grid sample layer that samples tokens from features and blank learnable embeddings. We show the embeddings that are used for each task in Table 1 detailedly.

***FIND* Interface** After the embeddings are prepared for each task, we define the task-specific attention mask for both content and conditional attention. Given arbitrary Input =  $\{f_a, \dots, f_z, t_a, \dots, t_z, p_a, \dots, p_z, q_a, \dots, q_z\}$ , the attention mask is a 2d binary matrix  $M_{\text{attn}}$  with shape  $[\text{len}(\text{input}), \text{len}(\text{input})]$ , where the positive attention region is defined in Table 1 in the columns of content attention and conditional attention. For example,  $q_{\text{image}} : f_{\text{image}}$  means the attention mask is positive in the direction of  $q_{\text{image}} \leftarrow f_{\text{image}}$  where image queries can see image features. As shown in Fig. 2, the *FIND* interface takes in only task-specific embeddings and attention masks and output queries and proposals for outputs. We will illustrate the detailed operation in Sec. 2.3.

**Projection** The outputs of *FIND* interface are a set of queries and proposals: Output =  $\{p_a, \dots, p_z, q_a, \dots, q_z\}$ . We then project the output using linear layers,  $L_{\text{semantic}}$  and  $L_{\text{pixel}}$ , to obtain semantic or pixel outputs:  $O_s = L_{\text{semantic}}(\text{Output})$ ,  $O_p = L_{\text{pixel}}(\text{Output})$ . The semantic outputs would be used for retrieval, and semantic mappings, while pixel outputs are used for mask prediction.

**Task Head** With the projected embeddings, each task can be represented as a similarity mapping procedure. The proposal masks ( $M_{\text{proposal}}$ ), proposal similarity scores ( $P_{\text{sim}}^{s,p}$ ), and query similarity scores ( $Q_{\text{sim}}^{s,p}$ ) are defined as:

$$P_{\text{sim}}^{s,p} \cup Q_{\text{sim}}^{s,m} = O^{\{s,p\}} \times O^{\{s,p\}} \quad (2)$$

$$M_{\text{proposal}} = O^p \times f_{\text{image}} \quad (3)$$

where we abuse the symbol of  $\cup$  to note  $P_{\text{sim}}^{s,p}$  and  $Q_{\text{sim}}^{s,p}$  are

Task	Embeddings			Operators		
	Proposals	Queries	Tokens	Content Attention	Condition Attention	Projection
Generic Segmentation	object	class	class	p.object:f.image q.class:t.class	p:p, q:q, t:t	Pixel, Semantic
Grounded Segmentation	grounding	description	description	p.grounding:f.image q.description:t.description	p:p, q:q, t:t p.grounding:t.description	Pixel, Semantic
Image-Text Retrieval	-	image, caption	caption	q.image:f.image q.caption:t.caption	p:p, q:q, t:t	Semantic
Interactive Segmentation	segment	spatial	spatial	p.segment:f.image q.spatial:t.spatial	p:p, q:q, t:t p.segment:t.spatial	Pixel, Semantic
Interleave Segmentation	entity	entity	interleave, .spatial	p.entity:f.image q.entity:t.interleave t.interleave:t.spatial	p:p, q:q, t:t p.entity:t.interleave	Pixel, Semantic
Interleave Retrieval	-	image, interleave	interleave, .spatial	q.image:f.image q.interleave:t.interleave t.interleave:t.spatial	p:p, q:q, t:t	Semantic

Table 1. Multi-Modal Interface. We define each task under the prototype of the interface that enables a shared embedding space, and a unified and flexible architecture for future tasks. Where  $p, q, t, f$  stands for proposals, queries, tokens, memories, and features. The colors red, blue, and yellow mean embeddings of vision, language and interleave modality. “y:x” denotes that in the attention module, the attention mask is visible between y and x in the unidirectional manner which means x is visible to y.

computed in the same way. For each task, the output is a combination of  $P_{sim}^{s,p}$ , and  $Q_{sim}^{s,p}$ , where the similarity scores define the selected proposals in  $P$ , or selected queries  $Q$  across the dataset. In addition, each proposal is associated with a mask, which gives pixel-level output for  $P_{sim}^{s,m}$ .

### 2.3. Interface Operators

The *FIND* Interface contains two main operators which are attention layers. *Content attention* defines the operation that gathers information through a certain search space defined by the attention mask, and *conditional attention* further constrains the search space. Here, when we mention gathering information, we denote the abstract procedure that proposals and queries are attending with corresponding features and tokens through attention layers. After which the proposals and queries are the weighted sum of corresponding features’ and tokens’ embeddings. We formally define the content and conditional attention as follows, in which the  $q, k, v$  are the same for each attention. As shown in Fig. 2 (b), the interface operators are a stack of modules that contain content and conditional attentions, thus we use  $\{.t$ , and  $\{.t+1$  to denote the current and next layer variables.

$$T_t, P_t, Q_t = \text{Cont\_Attn}([P_t, Q_t, F, T_t], M_a^t) \quad (4)$$

$$P_{t+1}, Q_{t+1}, T_{t+1} = \text{Cond\_Attn}([P_t, Q_t, T_t], M_a^d) \quad (5)$$

where  $\text{Cont\_Attn}$ , and  $\text{Cond\_Attn}$  are abbreviations of content and conditional attention, while  $M_a^t$ , and  $M_a^d$  denote attention mask for  $\text{Cont\_Attn}$  and  $\text{Cond\_Attn}$ .

Given the embeddings, pipeline, and operators defined above, we show the prototype for each task in Table. 1. To be more understandable, we give a case study for interleave segmentation under our prototypable framework.

### 2.4. Case Study: Interleave Segmentation

As shown in Table. 1, interleave segmentation takes use of both proposals and queries denoted as  $q.entity$  and  $p.entity$  that are sampled from the learnable embeddings, with the shape of  $[100, 512]$  and  $[n, 512]$ , where n is the total number of entities queried in the image. In addition, interleave segmentation also uses spatial and interleave tokens denoted by  $t.spatial$ ,  $t.interleave$ . The spatial tokens are sampled from image features  $f.image$  with  $t.spatial = \text{Embedding\_Sampler}(f.image, \text{coord})$ , where  $\text{coord}$  is the spatial mask coordinates.  $t.interleave$  is the identity mapping of  $f.text$ , where the spatial entities are represented with [INTERACTIVE]. We could formally define  $input = \{q.entity, p.entity, f.image, t.spatial, t.interleave\}$ . According to the operators’ column in Table. 1, we can represent the attention mask in the following format:

$$M_a^t = \begin{bmatrix} F & \mathbf{T} & F & F & F \\ F & F & F & F & \mathbf{T} \\ F & F & F & F & F \\ F & F & F & F & F \\ F & F & F & \mathbf{T} & F \end{bmatrix} M_a^d = \begin{bmatrix} \mathbf{T} & F & F & \mathbf{T} \\ F & \mathbf{T} & F & F \\ F & F & \mathbf{T} & F \\ F & F & F & \mathbf{T} \end{bmatrix} \quad (6)$$

The index of matrix coordinates follows the  $input$  order, and there is no  $f.image$  involved in  $M_a^d$ . The corresponding attention mask for each task is shown in Fig. 2 (c). We will then compute,  $P, Q = \text{FIND}(input, M_a^t, M_a^d)$ , where  $P = \{p.entity\}$ ,  $Q = \{q.entity\}$ . Then, we will project  $P, Q$  to the corresponding space with  $O_s = \{p_s.entity, q_s.entity\} = L_{semantic}(\{P, Q\})$ , and  $O_p = \{p_p.entity, q_p.entity\} = L_{pixel}(\{P, Q\})$ .

After we get the projected embeddings on semantic and pixel space, we could compute the similarity between queries and proposals:

$$P_{sim}^s = p_s.entity \times q_s.entity \quad (7)$$

$$M_{proposal} = p_p.entity \times f.image \quad (8)$$

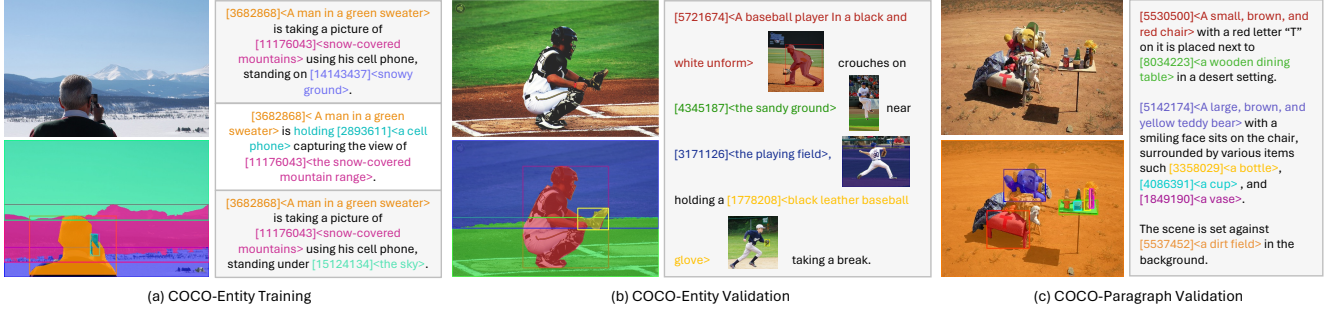


Figure 3. Example ground truth for FIND-Bench. (a) Grounded captions for COCO-Entity training set. (b) Grounded captions together with interleaved visual references for COCO-Entity validation set. (c) Grounded captions for COCO-Paragraph validation set. (The interleaved visual references are omitted due to space limit.)

### Algorithm 1 Pseudo code for Data Engine.

```

# Inputs: llava_cap, coco_cap, coco_pano, lvis_inst;
# Annotation of single image from multiple source.
1 def data_engine(llava_cap, coco_cap, coco_pano, lvis_inst):
2   Content = ``generate image captions with grounded
   entities and attributes with following:
   pseudo image description: <{}>,
   ground truth image captions: <{}>,
   ground truth bounding boxes (x0,y0,w,h): (x0,y0)
   is the top-left corner, (w,h) is box size),
   category_info, and entity_id: <{}>,
   entity_proposal: <{}>,
   an example output format would be: "(entity_id)<A
   woman> sitting next to (entity_id)<a handsome
   man>, with their hands holding together
   under (entity_id)<the blue sky>.", where
   (entity_id) and <xxx> are associated with the
   ground truth bounding boxes. entity_id is the
   real id number in the ground truth bounding
   boxes. generated caption constraints: 1. xxx;
   2. xxx; ''' .format(llava_cap, coco_cap, coco_pano,
   lvis_inst)) ;
3   output = GPT4(content)

```

where  $P_{sim}^s$  is the similarity between proposals and queries on semantic space with shape  $[100, n]$ , and  $M_{proposal}$  is the mask for each proposal. We compute the index for the proposal with  $P_{idx} = \text{argmax}(P_{sim}^s, \text{dim} = 1)$ . And the final output mask for interleaved segmentation is computed as  $M_{output} = M_{proposal}[P_{idx}]$ .

## 3. FIND Bench

In order to evaluate the capability of interleaved visual understanding, we propose a new benchmark called **FIND-Bench**. This includes a fully annotated dataset for both training and evaluation, featuring pairs of images and interleaved entity-based query, as shown in Fig. 3. FIND-Bench supports two new tasks, interleaved image retrieval and interleaved grounded segmentation, which we introduce in detail below.

### 3.1. Task Definition

**Interleaved Image Retrieval** let  $I$  and  $T$  denote, image, and text respectively. We define a search query as a se-

quence  $Q = \{q_1, q_2, \dots, q_n\}$ , where  $q_k$  can be either an instance of  $I_i$  or  $T_j$ . An example could be “A person with a red shirt is playing with [IMAGE] on the grassland.”, where [IMAGE] is an image. The search space, represented as  $S = \{I_1, I_2, \dots, I_m\}$ , is an image dataset.

**Interleaved Grounded Segmentation** Similar to interleaved image retrieval, we again define  $I$  as images,  $S, T$  as texts, where  $I, S$  represents entities (e.g. image reference, “a person”), and  $T$  represents text connections. The search query is formulated as a sequence  $Q = \{q_1, q_2, \dots, q_n\}$ ,  $q_i \in \{I, S, T\}$ . And the search space is all the segments for an image  $\{o_1, o_2, \dots, o_n\}$ . The objective is to find the corresponding  $o_i$  in the image for each instance of  $I, S$  in the query  $Q$ .

### 3.2. Dataset

**Data Engine** We create this new dataset on COCO images with ground truth labels, including captions and panoptic segmentation annotations. In addition, we leverage LLaVA [24] to generate detailed captions as instance-level pseudo-ground truth, and GPT4 as the augmentation engine. We show the pseudo-code of the data engine in Algo. 1, where GPT4 takes in all provided text information to generate entity-associated captions. Finally, we use SEEM to find the most visual-like cross-image instance for the labeled entity in each image. The pseudo-ground truths are verified by humans for quality control.

**Statistics** As shown in Table 2, our proposed dataset contains 118k training images, 5k validation images, together with 300k training captions, and 1000k training entities. Notably, each entity is associated with a bounding box, mask, phrase, or visual reference to support both text and interleaved grounding.

	Training			Evaluation			Entity Association		
	Images	Captions	Entities	Images	Captions	Entities	Mask	Phrase	Visual
COCO-Entity	118189	353219	1104907	4990	4990	15305	✓	✓	✓
COCO-Paragraph	-	-	-	4981	4981	22569	✓	✓	✓

Table 2. FIND-Bench statistics

	Data	Joint	Generic Segmentation			Grounded Segmentation					Interactive Segmentation			Image-Text Retrieval						
			COCO			RefCOCO-g		COCO-Entity		COCO-Paragraph		Pascal VOC			COCO-Karpathy		COCO-Entity		COCO-Paragraph	
			PQ	mAP	mIoU	cloU	mIoU	cloU	mIoU	cloU	mIoU	Point	Circle	Box	IR@1	TR@1	IR@1	TR@1	IR@1	TR@1
*Mask2Former (T) [7]	COCO (0.12M)	-	53.2	43.3	63.2	-	-	-	-	-	-	-	-	-	-	-	-	-	-	
*Mask2Former (B) [7]	COCO (0.12M)	-	56.4	46.3	67.1	-	-	-	-	-	-	-	-	-	-	-	-	-	-	
*Mask2Former (L) [7]	COCO (0.12M)	-	<b>57.8</b>	48.6	67.4	-	-	-	-	-	-	-	-	-	-	-	-	-	-	
Grounding-SAM (H) [25]	Grounding (5M)	✓	-	-	-	-	-	58.9	57.7	56.1	56.6	-	-	-	-	-	-	-	-	
SAM (B) [17]	SAM (11M)	-	-	-	-	-	-	-	-	-	-	58.2	-	61.8	-	-	-	-	-	
SAM (L) [17]	SAM (11M)	-	-	-	-	-	-	-	-	-	-	68.1	-	63.5	-	-	-	-	-	
*SEEM (T) [50]	COCO+LVIS (0.12M)	✗	50.8	39.7	62.2	60.9	65.7	54.3	56.1	52.6	54.6	83.5	86.0	71.8	-	-	-	-	-	
*SEEM (B) [50]	COCO+LVIS (0.12M)	✗	56.1	46.4	66.3	65.0	69.6	57.2	58.7	56.1	57.4	87.3	88.8	75.5	-	-	-	-	-	
*SEEM (L) [50]	COCO+LVIS (0.12M)	✗	57.5	47.7	<b>67.6</b>	65.6	70.3	54.8	57.8	53.8	56.7	88.5	<b>89.6</b>	76.5	-	-	-	-	-	
X-Decoder (T) [49]	COCO+HTP (4.12M)	✗	52.6	41.3	62.4	59.8	*	-	-	-	-	-	-	-	40.7/49.3	55.0/66.7	46.5/52.6	48.0/55.6	54.8/62.3	58.5/66.1
X-Decoder (B) [49]	COCO+HTP (4.12M)	✗	56.2	45.8	66.0	64.5	*	-	-	-	-	-	-	-	50.2/54.5	66.8/71.2	49.2/56.9	51.3/58.1	58.1/67.5	62.5/70.1
X-Decoder (L) [49]	COCO+HTP (4.12M)	✗	56.9	46.7	67.5	64.6	*	-	-	-	-	-	-	-	56.4/58.6	73.1/76.1	58.1/60.0	<b>59.9/62.7</b>	58.7/71.6	<b>72.0/74.1</b>
CLIP/ImageBind (H) [8, 12]	ITP (400M)	✓	-	-	-	-	-	-	-	-	-	-	-	-	49.4	65.9	53.4	57.6	59.6	64.8
FROMAGe (L) [18]	CC (12M)	✗	-	-	-	-	-	-	-	-	-	-	-	27.5	37.8	27.4	33.1	32.8	41.3	
BLIP-2 (L) [21]	COCO+HTP (130.1M)	✗	-	-	-	-	-	-	-	-	-	-	-	<b>63.4/59.1</b>	<b>74.4/65.2</b>	<b>59.1/58.8</b>	59.8/56.4	66.3/64.6	65.8/60.1	
FIND (T)	COCO (0.12M)	✓	51.0	42.3	62.0	61.1	65.3	68.5	62.5	65.0	59.4	84.3	85.8	74.5	40.4	53.0	51.0	51.5	61.2	62.9
FIND (B)	COCO (0.12M)	✓	55.5	49.0	65.7	65.3	69.3	69.5	63.0	<b>67.2</b>	60.1	86.3	88.0	75.0	45.8	60.6	56.3	56.7	65.5	69.1
FIND (L)	COCO (0.12M)	✓	56.7	<b>50.8</b>	67.4	<b>65.9</b>	<b>70.5</b>	<b>69.7</b>	<b>64.2</b>	66.6	<b>61.2</b>	<b>88.5</b>	89.5	<b>77.4</b>	46.3	61.9	57.2	58.2	<b>67.2</b>	68.6

Table 3. Benchmark on general multi-modal understanding tasks with one model Architecture with joint training for all. We compared the training dataset for each method, as well as whether the tasks are jointly trained for producing the results. \*Unlike X-Decoder and FIND, SEEM is trained with a deformable vision encoder. We report both the ensembled and the decoder retrieval results for X-Decoder (un-ensemble/ensemble), and we also report the finetuned and pre-trained results for blip2 (finetuned/pre-trained). Noted that we compute the ITC score for blip2 instead of ITM.

## 4. Experiment

**Datasets** We use COCO [23] as our main training and evaluation dataset which spans diverse annotation types. Apart from COCO-panoptic, we also make use of the annotation of Ref-COCO [26, 27, 43], COCO-Karpathy [16], and the proposed COCO-Entity dataset. Unless specified otherwise, our model is jointly trained on all tasks listed in Table 1.

**Settings** We benchmark our method on three different sizes, including the Tiny (FocalNet), Base (Davit-d3), and Large (Davit-d3) models. The vision backbone is reusing the X-Decoder pre-trained weight unless specified as SAM. The language pre-trained weight is LLaMa unless specified as UniCL. During training, we fixed the vision and language encoder and only train the FIND-Interface.

**Evaluation Metrics** We evaluate all the tasks with their standard evaluation metrics. For the newly proposed interleaved image retrieval task, we use IR@5, and IR@10 (Interleave-to-image Retrieval precision at rank 5/10) as the evaluation metrics. For interleaved grounded segmentation, we evaluate on cloU (pixel-wise IoU), and mIoU (image-wise IoU).

**Baselines** We evaluate ImageBind [12], FROMAGe [18], BLIP2 [21] for interleaved retrieval task; and Grounding-SAM [25] for interleaved (text-only) grounded segmentation on FIND-Bench. We try our best to design the pipeline to get the best performance for the baselines.

### 4.1. Main Results

In the main experiments, we evaluate the capability of *FIND* on both general multi-modal settings and interleaved settings.

**Comparison on standard multi-modal settings.** Table 3 compares *FIND* with strong baselines on generic segmentation tasks including panoptic segmentation, instance seg-

mentation, and semantic segmentation. In addition, we demonstrate the segmentation capability on both referring segmentation (RefCOCO-g: one sentence is associated with one instance) and grounded segmentation (COCO-Entity and COCO-Paragraph: one sentence is associated with multiple instances) settings. Moreover, we also benchmark *FIND*'s performance on image-text retrieval on three different ground truth types on COCO, where the average sentence length for the splits (Karpathy, Entity, and Paragraph) gradually increases. Below are the takeaways:

*The instance segmentation result stands out:* When compared with models of similar architecture, such as Mask2Former, X-Decoder, and SEEM, our approach with a large vision encoder performs extremely well on instance segmentation. It achieves a performance that is 2.2 points higher than Mask2Former (L), which makes use of deformable convolution as well. Note that the segmentation training data is identical between Mask2Former and *FIND*. The performance gain is likely because we have a fully unified segmentation and grounding pipeline so that the semantic ground truth from each domain is mutually beneficial.

*Grounded segmentation and referring segmentation are mutually beneficial:* In *FIND*, we formulate both grounded segmentation and referring segmentation in a unified way, so that a language description query is attended with language tokens to gather information spanning the language token range. Afterward, a similarity map is computed between the language description query and segment proposals. The matched proposal is finally used for predicting the mask. As shown in Table 3, in addition to state-of-the-art performances on both COCO-Entity and COCO-Paragraph, our model also achieves the best result over strong baselines on Ref-COCOg dataset, including SEEM which is trained with deformable convolution.

*Interactive segmentation performance is preserved in the*

	Interleave Segmentation						Interleave Retrieval				Generic Segmentation								
	COCO-Entity			COCO-Paragraph			COCO-Entity		COCO-Paragraph		Class			Visual Context			Description		
	cIoU	mIoU	AP50	cIoU	mIoU	AP50	IR@5	IR@10	IR@5	TR@5	PQ	mAP	mIoU	PQ	mAP	mIoU	PQ	mAP	mIoU
Mask2Former (L) [7]	-	-	-	-	-	-	-	-	-	57.8	48.6	67.4	-	-	-	-	-	-	
Grounding-SAM (H) [25]	58.9	57.7	63.2	56.1	56.6	62.5	-	-	-	-	-	-	-	-	-	-	-	-	
CLIP/ImageBind (H) [8, 12]	-	-	-	-	-	-	51.4	61.3	58.7	68.9	-	-	-	-	-	-	-	-	
FROMAGe (L) [18]	-	-	-	-	-	-	24.1	34.2	26.0	36.6	-	-	-	-	-	-	-	-	
BLIP-2 (L) [21]	-	-	-	-	-	-	20.8 / 34.3	25.8 / 47.7	22.1 / 39.3	27.1 / 54.7	-	-	-	-	-	-	-	-	
X-Decoder (T) [49]	-	-	-	-	-	-	23.6	32.2	25.6	35.5	52.6	41.3	62.4	-	-	-	18.5	15.9	22.5
X-Decoder (B) [49]	-	-	-	-	-	-	26.7	35.8	32.1	42.0	56.2	46.3	67.1	-	-	-	20.8	15.0	24.7
X-Decoder (L) [49]	-	-	-	-	-	-	26.8	36.2	32.2	43.4	57.8	48.6	67.4	-	-	-	23.5	21.1	21.7
SEEM (T) [50]	67.6	67.2	75.8	65.9	65.7	74.4	-	-	-	-	50.8	39.7	62.2	-	-	-	18.6	15.7	16.0
SEEM (B) [50]	69.4	69.2	77.8	69.2	68.6	77.3	-	-	-	-	56.1	46.4	66.3	-	-	-	22.9	21.6	20.0
SEEM (L) [50]	68.3	69.0	77.5	67.7	68.4	77.0	-	-	-	-	<b>56.9</b>	46.7	<b>67.5</b>	-	-	-	24.0	26.4	18.7
FIND (T)	74.9	68.1	79.5	73.2	66.4	77.7	43.5	57.1	49.4	63.9	51.0	42.3	62.0	41.8	32.3	51.6	19.5	30.2	<b>35.5</b>
FIND (B)	76.3	69.7	<b>81.8</b>	<b>75.1</b>	68.0	79.7	51.4	64.6	60.5	73.4	55.5	49.0	65.7	47.1	36.7	53.6	16.5	26.7	26.7
FIND (L)	<b>76.3</b>	<b>69.7</b>	81.7	74.7	<b>68.6</b>	<b>79.7</b>	<b>53.4</b>	<b>66.7</b>	<b>62.7</b>	<b>75.0</b>	56.7	<b>50.8</b>	67.4	<b>49.5</b>	<b>38.9</b>	<b>57.1</b>	<b>27.0</b>	<b>31.2</b>	26.8

Table 4. Benchmark on interleaved understanding with the jointly trained model with one set of weights. We conduct solid experiments on baselines approach ImageBind, FROMAGe, and BLIP-2, where we exhaustively try the best settings.

Vision	Language	Generic Segmentation						Grounding		Interactive		Retrieval	
		PQ	mAP	mIoU	Class	Description	mIoU	g-Ref	l-IoU	g-Ref	l-IoU	IR@1	TR@1
X-Decoder (T) [49]	UniCL [40]	48.5	39.0	61.4	12.4	20.7	18.9	61.3	82.6	40.4	54.0	-	-
X-Decoder (T) [49]	LLaMa [34]	48.5	38.9	61.2	19.5	30.2	35.5	61.6	82.5	40.2	52.2	-	-
SAM (B) [17]	UniCL [40]	42.5	37.6	53.6	4.5	17.7	17.9	64.9	81.6	29.1	39.5	-	-
SAM (B) [17]	LLaMa [34]	42.5	36.9	53.0	6.1	15.6	16.6	58.9	81.5	27.0	35.5	-	-

Table 5. Ablate on different foundation model architectures.

Task	COCO			g-Ref	Entity	VOC	Karpthy		Entity	
	PQ	mAP	mIoU				IR@1	TR@1	IR@1	TR@1
All	48.5	39.0	<b>61.4</b>	<b>61.3</b>	73.0	82.6	<b>40.4</b>	<b>54.0</b>	<b>50.8</b>	<b>51.9</b>
- Retrieval	48.5	39.0	61.1	60.6	<b>73.2</b>	<b>82.8</b>	-	-	44.3	44.8
- Grounding	48.6	39.1	61.3	-	40.9	82.8	-	-	45.3	46.2
- Interactive	48.6	38.8	61.0	-	36.5	-	-	-	31.4	33.4
- Interleave	<b>48.9</b>	<b>39.3</b>	61.0	-	-	-	-	-	-	-

Table 6. Ablate on each training task.

*unified settings.* Unlike SEEM which is only trained on image-only tasks, *FIND* is trained also on image-text tasks, such as image-text retrieval. With the splitting design of proposals and queries, the training in interactive segmentation and image-text retrieval is independent at the embedding level. Thus, it enables our approach to achieve competitive performances (i.e. *FIND* 88.5/89.5/77.4 vs. SEEM 88.5/89.6/76.5).

*The “less fascinating” results on image-text retrieval:* The main reason for the sub-optimal solution of our approach on image-text retrieval is caused by the batch size during finetuning. All the models are trained jointly for all the tasks, to create the interleaved shared embedding space between image, object, word, and sentence. Pilot experiments in X-Decoder have shown that training with different resolutions such as 1024 for image and 224 for language does not generalize well across granularities (e.g. 1024x1024 image will perform poorly on image text retrieval, 224x224 image cannot be well segmented). Thus, in *FIND*, we train our model with the same resolution for all tasks. In Table 3, all the models are either 384x384 with batch size 384 or 1024x1024 with batch size 192 for all tasks. Note that all other tables show results with the model with 640x640 training resolution and 192 batch size. Our approach achieves competitive performance on COCO-Entity and COCO-Paragraph compared with strong baselines.

**Compared with interleaved settings.** In Table 4, we eval-

Language Level	PQ	COCO			g-Ref	Entity	VOC	Karpthy		Entity	
		mAP	mIoU	cIoU				IR@1	TR@1	IR@1	TR@1
[-1]	48.3	39.1	61.2	61.3	73.0	82.6	38.9	52.2	50.3	50.8	
[-6]	47.8	38.8	60.4	60.3	72.9	81.3	38.1	49.9	48.1	47.5	
[-12]	<b>48.5</b>	<b>39.0</b>	<b>61.4</b>	61.3	<b>73.0</b>	<b>82.6</b>	<b>40.4</b>	<b>54.0</b>	<b>50.8</b>	<b>51.9</b>	
[-18]	48.2	39.0	61.1	62.2	72.6	82.2	40.1	52.7	50.6	50.5	
[-24]	48.5	38.8	61.5	<b>61.6</b>	72.9	82.6	40.2	52.2	50.5	51.3	
[-30]	48.1	39.2	61.1	60.1	73.3	82.4	37.9	49.3	49.4	50.0	

Table 7. Ablate on LLM feature layers.

uate *FIND* on the interleaved image and pixel level understanding tasks on *FIND*-Bench. Different from COCO-Entity and COCO-Paragraph in Table 3, the entity in the text is randomly replaced with visual content with 0.5 probability.

*Interleaved Segmentation:* We build an interleaved segmentation baseline using the SEEM model. Instead of formulating the grounding task in a sentence that SEEM doesn’t support, we simply separately infer each entity for either interactive or grounding for SEEM. As shown in Table 4, *FIND* outperforms SEEM with around +8 points on both COCO-Entity and COCO-Paragraph under cIoU metrics.

*Interleaved Retrieval:* Apart from interleaved segmentation capability at the image level, we also explore the cross-image interleaved retrieval capability that is a zero-shot task to the current settings. As the interleaved reference objects are also selected from COCO val2017 sets, IR@1 is not meaningful, thus we only report IR@5 and IR@10 results. For ImageBind and BLIP-2, we use the ensemble scores of all the texts, sentences, and images. We follow the original settings of FROMAGe to perform interleaved image-text retrieval. Our performance is substantially higher than the proposed baselines, which again indicates the effectiveness of our interleaved shared embedding space.

*Generic Segmentation:* In addition to the classic evaluation on generic segmentation with class names or fixed index, here we replace the categories with either class descriptions (a long description without the corresponding class name) or visual prompts (an average feature for the object embeddings in each class). With the benefit of LLMs, *FIND* can perform much better on description-based generic segmentation. This is quite intuitive, that a large language model has a smoother representation when describing the same

thing in multiple ways. In addition, an LLM is better at dealing with long context. In addition, we also showcase that *FIND* is usable in the visual context setting.

## 4.2. Ablation Study

We ablate our approach in three perspectives: (1) How well the proposed interface is generalized to different foundation models. (2) What is the effectiveness of each task in the unified pipeline. (3) The effectiveness of using intermediate layers of the LLM representation.

*Apply to different foundation models architectures:* In the main experiments, we use X-Decoder as the vision encoder, and LLaMA as the language encoder, which shows convening performance on all the benchmarks. X-Decoder has been trained to pair up vision and language embeddings, however, SAM is only trained on segmentation data without any semantic meaning. Thus, we use SAM as an ablation foundation model, to study how important is vision encoder trained with semantic data. For the language encoder, we adopt UniCL which has the same size as Bert to study the difference between a standard language encoder, and an LLM encoder. As shown in Table 5, UniCL and LLaMA usually have very similar performance with X-Decoder as vision encoder, except that LLaMA is extremely effective for language description. Although the performance of SAM is much worse than its counterpart X-Decoder on semantic understanding after aligning the interface, our approach also shows that without any modification to SAM, it applies to semantic understanding tasks on generic, grounded segmentation, and image-text retrieval.

*Independent task effectiveness:* We explore the independent task effectiveness by gradually removing a task in Table 6. Removing image-text retrieval will hurt the interleave retrieval performance (we actually don't train with cross-image visual prompts) by a great margin. Additionally, further removing the grounding task will also decrease the performance of the entity-based grounding task. As interleave grounding is highly related to interactive segmentation, removing interactive segmentation will also decrease the interleave segmentation performance. Last, when only panoptic segmentation is trained, the performance is very similar to other settings, which indicates that the unified interface is consistent with the procedure training the basic understanding task.

*Varying the feature embeddings layer for LLM:* The large language model takes in language tokens as input and outputs the generated text based on the input contents. Thus, it is easy to think that the LLM embeddings would be less semantic near both the input and output layers. However, we believe that the intermediate feature layers would be best aligned with vision embeddings that are highly clustered and semantic. In Table 7, we study the performance across generic segmentation, grounding, and image-texture

retrieval with features from layer -1 (close to output) to layer -30 (close to input). We can observe that the features at layer -12 have the best performance, and both the top and bottom layers are much worse for image-text retrieval on COCO-Karparthy splits. Throughout the paper, we use -12 layer features for LLaMA.

## 4.3. Qualitative Results

We qualitatively demonstrate the effectiveness of our approach in Fig. 1 and Fig. 4. Fig. 1 demonstrates that generic segmentation using *FIND* is able to handle complex scenes. Notably, the picnic image for generic segmentation is generated from Dalle-3, which indicates that our approach is working on both in-domain and out-of-domain images. Further, sometimes we may not exactly know the exact word that we want to reference, thus we also show that our model works well with complex descriptions. The model is also able to maintain the interactive segmentation capability.

On the interleaved image retrieval settings, we show that our model is able to find both visually similar and context-related images. For example, using a black dog as an example will tend to retrieve images that contain black dogs, and the same for white dogs. In addition, the vision and language query is also exchangeable, where changing a bench to a chair image is able to retrieve the result that has the exact matched instance.

In addition, although we never trained with language grounding, our model can generalize to interleaved phrase grounding in that image, and the text can find the exact grounded phrases in the long paragraph.

## 5. Related Works

**Foundation Models.** Recent years have seen a speedy evolution of foundation models in diverse areas such as computer vision [44], natural language processing [3, 9, 29, 35], and their interactions [1, 21, 42]. For example, GPT-3 [3] heralds breakthroughs in natural language understanding and generation tasks, like text completion, translation, summarization, and question answering. As a vision foundation model, Florence [39, 44] can be easily adapted for various computer vision tasks, such as classification, retrieval, object detection, VQA, image captioning, video retrieval, and action recognition. Flamingo [1] bridges powerful pre-trained vision-only and language-only models by token fusion with cross-attention. BLIP-2 [21] proposes an efficient pretraining strategy that bootstraps vision-language pre-training with a lightweight Q-Former in two stages.

Given those different foundation models in various modalities, we believe that LLMs and vision models can be unified in the embedding space. Different from previous multi-modal approaches, such as Flamingo [1], LLaVa [24] and Q-Former (BLIP-2) [21] that feed the vision foundation model output into a language decoder and use the LLM



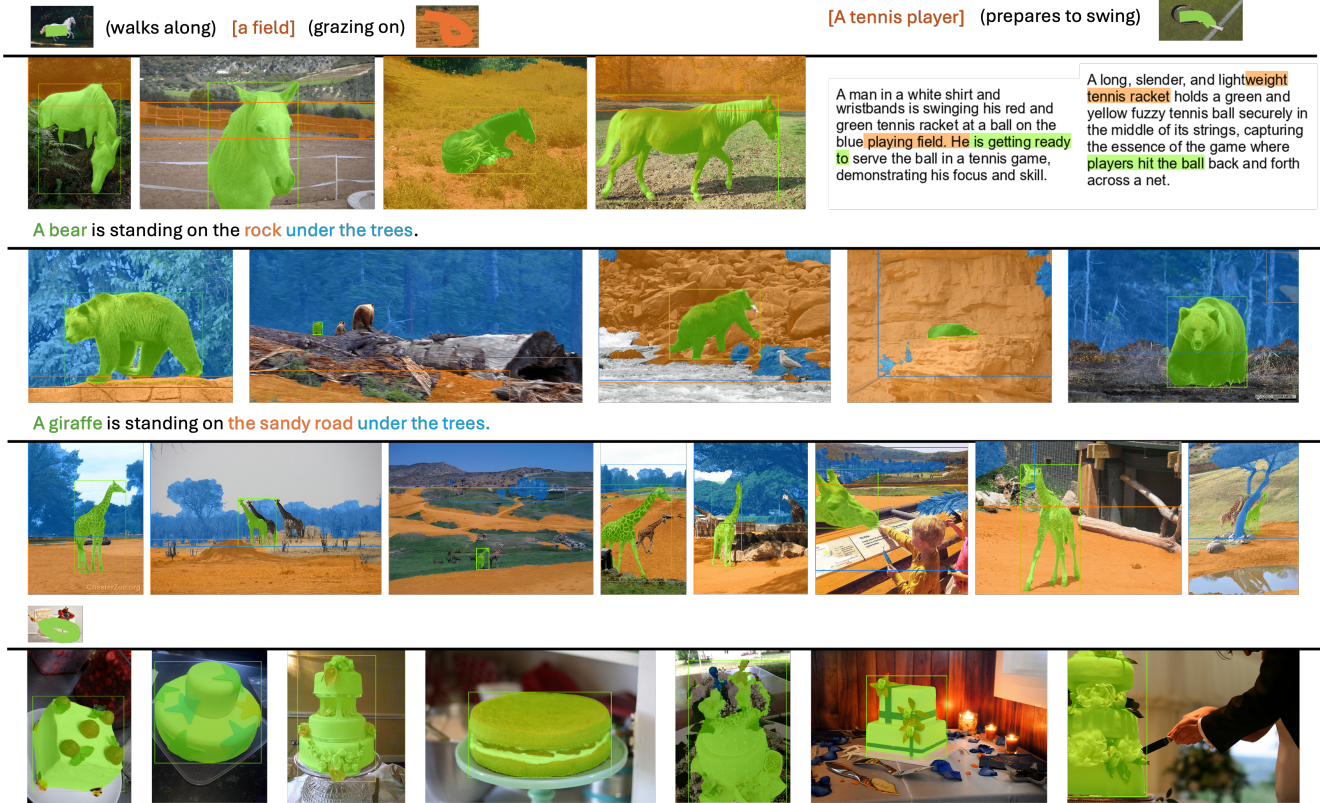


Figure 4. Qualitative results on interleave segmentation and retrieval.

as an interpreter, our goal is to interface foundation model embeddings.

**Interleaved Image-Text Understanding.** Previous works have explored interleaved visual understanding in the context of visual question answering, visual dialogue, image captioning, and interleaved image retrieval [1, 12, 18]. In addition, recent works [45] have also explored contextual detection that associates phrases with visual content in a sentence. However, although these works reveal interleave capability on image understanding, they lack an evaluation benchmark, as well as a complete training dataset. Though [2, 19, 48] have proposed a new benchmark on interleaved generation and understanding of image and document level, there is no one available for the interleaved tasks between interactive image parts and phrases.

To this end, we introduce the interleaved segmentation and interleaved retrieval tasks with our carefully designed benchmark *FIND*-Bench. We further propose our approach which uses masked attention to control different tasks, and we prototype the attention procedure following the protocol, with adaptive retrieval, segmentation, and grounding in the interleaved manner. Compared to works that use masked attention [21, 50] to fuse the vision output and LLM input, we care more about interfacing and unifying foundation models’ embeddings, i.e., an LLM acts as both the encoder

and decoder.

**Image Understanding.** Vision Transformers [11, 14, 15, 30–33, 36, 38, 46] have dominated a wide range of key image understanding tasks, such as image retrieval, detection, and segmentation, by applying self-attention to a sequence of image patches. Previously, multimodal methods [6, 22, 47] solve the retrieval tasks pretty well. However, they are not able to handle pixel-level understanding tasks, like instance segmentation. On the other hand, open-vocabulary segmentation methods have recently drawn much attention, including generic segmentation [5, 10, 50], interactive segmentation [13, 17] that separates objects by actively integrating user inputs, and grounded segmentation [49, 50] that grounds object segments from language descriptions. In this work, we propose *FIND* as a unified interface that can support all the above tasks, while maintaining decent performance, and further enabling two new tasks interleaved segmentation and interleaved retrieval. We unify these tasks by interfacing foundation models’ embeddings.

## 6. Conclusions and Future Directions

This work proposes *FIND*, a generalized interface for aligning foundation models’ embeddings, which is widely generalizable, prototypable, interleavable, and highly extendable. We further introduce *FIND*-Bench, which introduces

new training and evaluation ground truth for two new tasks: interleaved segmentation and interleaved retrieval. Extensive evaluations on *FIND-Bench* and various widely-used benchmarks show the superiority of our approach on interleaved understanding benchmarks and its competitiveness on standard retrieval and segmentation settings.

In the future, we can further extend *FIND* by 1) Integrating novel foundational models, e.g., investigating new instruction-based language encoders or new generative base vision encoders. 2) Exploring more cross-modal tasks, e.g., interleaved image/video generation tasks and language generation with multi-round capabilities, given the interleave capability extends to visual generation. 3) Extension to long context, e.g., extending language to paragraph-wise understanding and extending vision to database-wise understanding. 4) Extending object queries to different granularities in a more flexible manner.

**Broader Impact.** Our work is of broad interest to the vision and language community. Our proposed approach has no new ethical or social issues on its own, except those inherited from foundational models.

## 7. Acknowledgement

This work was supported in part by NSF CAREER IIS2150012, NASA 80NSSC21K0295, the Institute of Information and communications Technology Planning and Evaluation (IITP) grant funded by the Korea government (MSIT) (No. 2022-0-00871, Development of AI Autonomy and Knowledge Enhancement for AI Agent Collaboration).

## References

- [1] Jean-Baptiste Alayrac, Jeff Donahue, Pauline Luc, Antoine Miech, Iain Barr, Yana Hasson, Karel Lenc, Arthur Mensch, Katherine Millican, Malcolm Reynolds, et al. Flamingo: a visual language model for few-shot learning. *Advances in Neural Information Processing Systems*, 35:23716–23736, 2022. 8, 9
- [2] Jie An, Zhengyuan Yang, Linjie Li, Jianfeng Wang, Kevin Lin, Zicheng Liu, Lijuan Wang, and Jiebo Luo. Openleaf: Open-domain interleaved image-text generation and evaluation. *arXiv preprint arXiv:2310.07749*, 2023. 9
- [3] Tom Brown, Benjamin Mann, Nick Ryder, Melanie Subbiah, Jared D Kaplan, Prafulla Dhariwal, Arvind Neelakantan, Pranav Shyam, Girish Sastry, Amanda Askell, et al. Language models are few-shot learners. *Advances in neural information processing systems*, 33:1877–1901, 2020. 8
- [4] Sébastien Bubeck, Varun Chandrasekaran, Ronen Eldan, Johannes Gehrke, Eric Horvitz, Ece Kamar, Peter Lee, Yin Tat Lee, Yuanzhi Li, Scott Lundberg, et al. Sparks of artificial general intelligence: Early experiments with gpt-4. *arXiv preprint arXiv:2303.12712*, 2023. 2
- [5] Liang-Chieh Chen, George Papandreou, Florian Schroff, and Hartwig Adam. Rethinking atrous convolution for semantic image segmentation. *arXiv preprint arXiv:1706.05587*, 2017. 9
- [6] Yen-Chun Chen, Linjie Li, Licheng Yu, Ahmed El Kholy, Faisal Ahmed, Zhe Gan, Yu Cheng, and Jingjing Liu. UNITER: universal image-text representation learning. In *ECCV*, pages 104–120, 2020. 9
- [7] Bowen Cheng, Ishan Misra, Alexander G Schwing, Alexander Kirillov, and Rohit Girdhar. Masked-attention mask transformer for universal image segmentation. In *Proceedings of the IEEE/CVF conference on computer vision and pattern recognition*, pages 1290–1299, 2022. 6, 7
- [8] Mehdi Cherti, Romain Beaumont, Ross Wightman, Mitchell Wortsman, Gabriel Ilharco, Cade Gordon, Christoph Schuhmann, Ludwig Schmidt, and Jenia Jitsev. Reproducible scaling laws for contrastive language-image learning. In *Proceedings of the IEEE/CVF Conference on Computer Vision and Pattern Recognition*, pages 2818–2829, 2023. 6, 7
- [9] Jacob Devlin, Ming-Wei Chang, Kenton Lee, and Kristina Toutanova. Bert: Pre-training of deep bidirectional transformers for language understanding. In *NAACL-HLT (1)*, 2019. 8
- [10] Mingyu Ding, Xiaochen Lian, Linjie Yang, Peng Wang, Xiaojie Jin, Zhiwu Lu, and Ping Luo. Hr-nas: Searching efficient high-resolution neural architectures with lightweight transformers. In *Proceedings of the IEEE/CVF conference on computer vision and pattern recognition*, pages 2982–2992, 2021. 9
- [11] Mingyu Ding, Bin Xiao, Noel Codella, Ping Luo, Jingdong Wang, and Lu Yuan. Davit: Dual attention vision transformers. In *European Conference on Computer Vision*, pages 74–92. Springer, 2022. 9
- [12] Rohit Girdhar, Alaaeldin El-Nouby, Zhuang Liu, Mannat Singh, Kalyan Vasudev Alwala, Armand Joulin, and Ishan Misra. Imagebind: One embedding space to bind them all. In *Proceedings of the IEEE/CVF Conference on Computer Vision and Pattern Recognition*, pages 15180–15190, 2023. 6, 7, 9
- [13] Leo Grady. Random walks for image segmentation. *IEEE transactions on pattern analysis and machine intelligence*, 28(11):1768–1783, 2006. 9
- [14] Benjamin Graham, Alaaeldin El-Nouby, Hugo Touvron, Pierre Stock, Armand Joulin, Hervé Jégou, and Matthijs Douze. Levit: a vision transformer in convnet’s clothing for faster inference. In *ICCV*, pages 12259–12269, 2021. 9
- [15] Byeongho Heo, Sangdoon Yun, Dongyoon Han, Sanghyuk Chun, Junsuk Choe, and Seong Joon Oh. Rethinking spatial dimensions of vision transformers. In *ICCV*, pages 11936–11945, 2021. 9
- [16] Andrej Karpathy and Li Fei-Fei. Deep visual-semantic alignments for generating image descriptions. In *Proceedings of the IEEE conference on computer vision and pattern recognition*, pages 3128–3137, 2015. 6
- [17] Alexander Kirillov, Eric Mintun, Nikhila Ravi, Hanzi Mao, Chloe Rolland, Laura Gustafson, Tete Xiao, Spencer Whitehead, Alexander C Berg, Wan-Yen Lo, et al. Segment anything. *arXiv preprint arXiv:2304.02643*, 2023. 2, 6, 7, 9

- [18] Jing Yu Koh, Ruslan Salakhutdinov, and Daniel Fried. Grounding language models to images for multimodal inputs and outputs. 2023. [2](#), [6](#), [7](#), [9](#)
- [19] Hugo Laurençon, Lucile Saulnier, Léo Tronchon, Stas Bekman, Amanpreet Singh, Anton Lozhkov, Thomas Wang, Siddharth Karamcheti, Alexander M Rush, Douwe Kiela, et al. Obelics: An open web-scale filtered dataset of interleaved image-text documents. In *Thirty-seventh Conference on Neural Information Processing Systems Datasets and Benchmarks Track*, 2023. [9](#)
- [20] Chunyuan Li, Zhe Gan, Zhengyuan Yang, Jianwei Yang, Linjie Li, Lijuan Wang, and Jianfeng Gao. Multimodal foundation models: From specialists to general-purpose assistants. *arXiv preprint arXiv:2309.10020*, 1:2, 2023. [2](#)
- [21] Junnan Li, Dongxu Li, Silvio Savarese, and Steven Hoi. Blip-2: Bootstrapping language-image pre-training with frozen image encoders and large language models. *arXiv preprint arXiv:2301.12597*, 2023. [2](#), [6](#), [7](#), [8](#), [9](#)
- [22] Xiujun Li, Xi Yin, Chunyuan Li, Pengchuan Zhang, Xiaowei Hu, Lei Zhang, Lijuan Wang, Houdong Hu, Li Dong, Furu Wei, Yejin Choi, and Jianfeng Gao. Oscar: Object-semantics aligned pre-training for vision-language tasks. In *ECCV*, pages 121–137, 2020. [9](#)
- [23] Tsung-Yi Lin, Michael Maire, Serge Belongie, James Hays, Pietro Perona, Deva Ramanan, Piotr Dollár, and C Lawrence Zitnick. Microsoft coco: Common objects in context. In *Computer Vision—ECCV 2014: 13th European Conference, Zurich, Switzerland, September 6–12, 2014, Proceedings, Part V 13*, pages 740–755. Springer, 2014. [2](#), [6](#)
- [24] Haotian Liu, Chunyuan Li, Qingyang Wu, and Yong Jae Lee. Visual instruction tuning. *arXiv preprint arXiv:2304.08485*, 2023. [2](#), [5](#), [8](#)
- [25] Shilong Liu, Zhaoyang Zeng, Tianhe Ren, Feng Li, Hao Zhang, Jie Yang, Chunyuan Li, Jianwei Yang, Hang Su, Jun Zhu, et al. Grounding dino: Marrying dino with grounded pre-training for open-set object detection. *arXiv preprint arXiv:2303.05499*, 2023. [6](#), [7](#)
- [26] Junhua Mao, Jonathan Huang, Alexander Toshev, Oana Camburu, Alan L Yuille, and Kevin Murphy. Generation and comprehension of unambiguous object descriptions. In *Proceedings of the IEEE conference on computer vision and pattern recognition*, pages 11–20, 2016. [6](#)
- [27] Varun K Nagaraja, Vlad I Morariu, and Larry S Davis. Modeling context between objects for referring expression understanding. In *Computer Vision—ECCV 2016: 14th European Conference, Amsterdam, The Netherlands, October 11–14, 2016, Proceedings, Part IV 14*, pages 792–807. Springer, 2016. [6](#)
- [28] OpenAI. Improving image generation with better captions. Technical report, OpenAI, 2023. [2](#)
- [29] OpenAI. Gpt-4 technical report. Technical report, OpenAI, 2023. [2](#), [8](#)
- [30] Carlos Riquelme, Joan Puigcerver, Basil Mustafa, Maxim Neumann, Rodolphe Jenatton, André Susano Pinto, Daniel Keysers, and Neil Houlsby. Scaling vision with sparse mixture of experts. *NeurIPS*, 34, 2021. [9](#)
- [31] Michael S. Ryoo, AJ Piergiovanni, Anurag Arnab, Mostafa Dehghani, and Anelia Angelova. Tokenlearner: What can 8 learned tokens do for images and videos? *arXiv: Computer Vision and Pattern Recognition*, 2021.
- [32] Aravind Srinivas, Tsung-Yi Lin, Niki Parmar, Jonathon Shlens, Pieter Abbeel, and Ashish Vaswani. Bottleneck transformers for visual recognition. In *CVPR*, pages 16519–16529, 2021.
- [33] Hugo Touvron, Matthieu Cord, Matthijs Douze, Francisco Massa, Alexandre Sablayrolles, and Hervé Jégou. Training data-efficient image transformers & distillation through attention. In *International Conference on Machine Learning*, pages 10347–10357. PMLR, 2021. [9](#)
- [34] Hugo Touvron, Thibaut Lavril, Gautier Izacard, Xavier Martinet, Marie-Anne Lachaux, Timothée Lacroix, Baptiste Rozière, Naman Goyal, Eric Hambro, Faisal Azhar, et al. Llama: Open and efficient foundation language models. *arXiv preprint arXiv:2302.13971*, 2023. [2](#), [7](#)
- [35] Ashish Vaswani, Noam Shazeer, Niki Parmar, Jakob Uszkoreit, Llion Jones, Aidan N Gomez, Łukasz Kaiser, and Illia Polosukhin. Attention is all you need. In *NeurIPS*, 2017. [8](#)
- [36] Wenhai Wang, Enze Xie, Xiang Li, Deng-Ping Fan, Kaitao Song, Ding Liang, Tong Lu, Ping Luo, and Ling Shao. Pyramid vision transformer: A versatile backbone for dense prediction without convolutions. In *ICCV*, 2021. [9](#)
- [37] Wenhai Wang, Zhe Chen, Xiaokang Chen, Jiannan Wu, Xizhou Zhu, Gang Zeng, Ping Luo, Tong Lu, Jie Zhou, Yu Qiao, et al. Visionllm: Large language model is also an open-ended decoder for vision-centric tasks. *arXiv preprint arXiv:2305.11175*, 2023. [2](#)
- [38] Kan Wu, Houwen Peng, Minghao Chen, Jianlong Fu, and Hongyang Chao. Rethinking and improving relative position encoding for vision transformer. In *ICCV*, pages 10033–10041, 2021. [9](#)
- [39] Bin Xiao, Haiping Wu, Weijian Xu, Xiyang Dai, Houdong Hu, Yumao Lu, Michael Zeng, Ce Liu, and Lu Yuan. Florence-2: Advancing a unified representation for a variety of vision tasks. *arXiv preprint arXiv:2311.06242*, 2023. [8](#)
- [40] Jianwei Yang, Chunyuan Li, Pengchuan Zhang, Bin Xiao, Ce Liu, Lu Yuan, and Jianfeng Gao. Unified contrastive learning in image-text-label space. In *Proceedings of the IEEE/CVF Conference on Computer Vision and Pattern Recognition*, pages 19163–19173, 2022. [7](#)
- [41] Jianwei Yang, Hao Zhang, Feng Li, Xueyan Zou, Chunyuan Li, and Jianfeng Gao. Set-of-mark prompting unleashes extraordinary visual grounding in gpt-4v. *arXiv preprint arXiv:2310.11441*, 2023. [2](#)
- [42] Lewei Yao, Runhui Huang, Lu Hou, Guansong Lu, Minzhe Niu, Hang Xu, Xiaodan Liang, Zhenguo Li, Xin Jiang, and Chunjing Xu. FILIP: fine-grained interactive language-image pre-training. In *ICLR*, 2022. [8](#)
- [43] Licheng Yu, Patrick Poirson, Shan Yang, Alexander C Berg, and Tamara L Berg. Modeling context in referring expressions. In *Computer Vision—ECCV 2016: 14th European Conference, Amsterdam, The Netherlands, October 11–14, 2016, Proceedings, Part II 14*, pages 69–85. Springer, 2016. [6](#)
- [44] Lu Yuan, Dongdong Chen, Yi-Ling Chen, Noel Codella, Xiyang Dai, Jianfeng Gao, Houdong Hu, Xuedong Huang,

- Boxin Li, Chunyuan Li, et al. Florence: A new foundation model for computer vision. *arXiv preprint arXiv:2111.11432*, 2021. 8
- [45] Yuhang Zang, Wei Li, Jun Han, Kaiyang Zhou, and Chen Change Loy. Contextual object detection with multimodal large language models. *arXiv preprint arXiv:2305.18279*, 2023. 9
- [46] Xiaohua Zhai, Alexander Kolesnikov, Neil Houlsby, and Lucas Beyer. Scaling vision transformers. *arXiv: Computer Vision and Pattern Recognition*, 2021. 9
- [47] Pengchuan Zhang, Xiujun Li, Xiaowei Hu, Jianwei Yang, Lei Zhang, Lijuan Wang, Yejin Choi, and Jianfeng Gao. Vinvl: Making visual representations matter in vision-language models. *arXiv preprint arXiv:2101.00529*, 2021. 9
- [48] Wanrong Zhu, Jack Hessel, Anas Awadalla, Samir Yitzhak Gadre, Jesse Dodge, Alex Fang, Youngjae Yu, Ludwig Schmidt, William Yang Wang, and Yejin Choi. Multimodal c4: An open, billion-scale corpus of images interleaved with text. *arXiv preprint arXiv:2304.06939*, 2023. 9
- [49] Xueyan Zou, Zi-Yi Dou, Jianwei Yang, Zhe Gan, Linjie Li, Chunyuan Li, Xiyang Dai, Harkirat Behl, Jianfeng Wang, Lu Yuan, et al. Generalized decoding for pixel, image, and language. In *Proceedings of the IEEE/CVF Conference on Computer Vision and Pattern Recognition*, pages 15116–15127, 2023. 6, 7, 9
- [50] Xueyan Zou, Jianwei Yang, Hao Zhang, Feng Li, Linjie Li, Jianfeng Gao, and Yong Jae Lee. Segment everything everywhere all at once. *arXiv preprint arXiv:2304.06718*, 2023. 3, 6, 7, 9